Journal of
Applied Crystallography
ISSN 0021-8898
Editor: **Anke R. Pyzalla**

New measures of sharpness for symmetric powder diffraction peak profiles

Takashi Ida

J. Appl. Cryst. (2008). **41**, 393–401

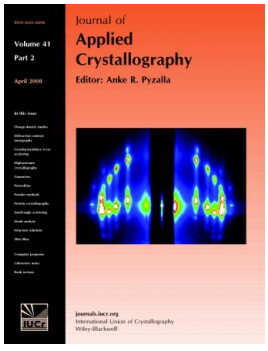

Journal of
Applied Crystallography
ISSN 0021-8898

Received 21 May 2007
Accepted 19 December 2007

New measures of sharpness for symmetric powder diffraction peak profiles

Takashi Ida

Ceramics Research Laboratory, Nagoya Institute of Technology, Asahigaoka, Tajimi 507-0071, Japan. Correspondence e-mail: ida.takashi@nitech.ac.jp

New measures of sharpness for symmetric powder diffraction peak profiles are proposed. The sharpness parameter is defined through the νth-order moment of the Fourier transform of the profile function. Analytical expressions for the sharpness parameter for empirical model profile functions, namely the Gaussian, logistic distribution, hyperbolic secant, Lorentzian, Voigt, Pearson VII and pseudo-Voigt functions, and theoretical size-broadening profiles with statistical size distribution are presented. Theoretical diffraction profiles with complicated formulae can be approximated by empirical model functions assuming equivalent values of the sharpness parameter. The concept of the sharpness parameter provides a simple way to define an approximation for a theoretical diffraction peak profile with empirical model functions.

1. Introduction

The main features of powder diffraction peaks are specified by (i) the integrated intensity, (ii) the peak position, (iii) the line width, (iv) the asymmetry and (v) the sharpness of the profile. Only the integrated intensities of the peaks are necessary to determine the most probable average crystallographic structure, while precise evaluation of peak positions is also important to determine the dimensions of the unit cell, which can be the deciding factor in identifying the crystallographic symmetry from powder diffraction data. Since the intrinsic line width of a diffraction peak is related to the coherence length along the diffraction vector, it can be used as a direct measure of the crystallinity along the corresponding crystallographic direction. Asymmetry of experimental peak profiles is usually attributed to instrumental aberrations or asymmetric spectroscopic distribution of the source X-rays.

Hereafter, we restrict our attention to a normalized symmetric peak profile function $f(k)$ located at the origin, for which the following equations hold:

$$\int_{-\infty}^{\infty} f(k)\,\mathrm{d}k = 1, \tag{1}$$

$$f(k) = f(-k). \tag{2}$$

Recently, Langford *et al.* (2000) have reported that the sharpness of the intrinsic diffraction peak profile is related to the distribution of the crystallite size, and suggested the ratio (B/W) of the integral breadth B, given by

$$B = 1/f(0), \tag{3}$$

for the normalized peak profile function $f(k)$, to the FWHM W, defined by

$$f(W/2) = f(0)/2$$

or

$$W = 2f^{-1}[f(0)/2], \tag{4}$$

as a measure of the sharpness of a symmetric powder diffraction peak profile. However, it is generally difficult to obtain an explicit formula of FWHM for a statistically distributed size-broadening profile.

The author has previously proposed the ratio (A/B) of the Fourier initial slope, defined by

$$A = -\lim_{x\to+0}\frac{\mathrm{d}}{\mathrm{d}x}\int_{-\infty}^{\infty} f(k)\exp(2\pi ikx)\,\mathrm{d}k, \tag{5}$$

to the integral breadth B to be used as a measure of sharpness (Ida *et al.*, 2003); this approach is consistent with the simultaneous application of two major conventional methods for line-broadening analysis, the Warren–Averbach (Warren, 1969) and Williamson–Hall (Williamson & Hall, 1953) methods, and is similar to the method applied by Ungár *et al.* (2001). It has also been shown that both A and B can easily be evaluated for the log-normally distributed size-broadening profile for a given median and logarithmic standard deviation.

Sánchez-Bajo *et al.* (2006) have pointed out that the use of the parameter (A/B) may cause systematic deviation on application of curve fitting analysis with the pseudo-Voigt function to the size-broadening profile. It has been shown that the pseudo-Voigt profile optimized to approximate the size-broadening profile has less sharpness than that determined by the same (A/B). Even though the validity of the approximation using the pseudo-Voigt profile has not yet been fully certified, it should be worth examining other measures for the sharpness of peak profile, which can provide a straightforward method to define an approximation for the size-broadening profile with empirical model profile functions.

In this paper, the author defines another type of line-width parameter, C_ν, with a tuneable parameter ν through the νth-order moment of the Fourier transform, and examines the validity of using the ratio of the integral breadth to this width parameter, (B/C_ν), as a measure of sharpness for a powder diffraction peak profile.

2. Definition of line-width parameter

If the cumulants of a peak profile function are defined up to the fourth order, the sharpness can be unambiguously determined by the kurtosis, which is given by the ratio of the fourth-order cumulant to the squared second-order cumulant of the function. The ith cumulant of a function $f(k)$ is defined by

$$\kappa_i = \lim_{\theta\to 0} \frac{\mathrm{d}^i}{\mathrm{d}\theta^i} \ln \int_{-\infty}^{\infty} \exp(\theta k) f(k)\,\mathrm{d}k.$$

When the function $f(k)$ is assumed to be normalized for simplicity, the zeroth cumulant is zero ($\kappa_0 = 0$), the first-order cumulant is identical to the mean position given by

$$\kappa_1 = \int_{-\infty}^{\infty} k f(k)\,\mathrm{d}k,$$

the second-order cumulant is identical to the variance given by

$$\kappa_2 = \int_{-\infty}^{\infty} (k-\kappa_1)^2 f(k)\,\mathrm{d}k,$$

and the third-order cumulant is identical to the third-order central moment given by

$$\kappa_3 = \int_{-\infty}^{\infty} (k-\kappa_1)^3 f(k)\,\mathrm{d}k.$$

The skewness, which can be used as a measure of asymmetry of peak profile, is defined as the ratio of the third-order cumulant to the cubic standard deviation, $\kappa_3/\kappa_2^{3/2}$. The fourth-order cumulant of the normalized function $f(k)$ is given by

$$\kappa_4 = \int_{-\infty}^{\infty} (k-\kappa_1)^4 f(k)\,\mathrm{d}k - 3\kappa_2^2,$$

and the kurtosis, which can be a measure of the sharpness of the peak shape, is defined as κ_4/κ_2^2.

However, it is well known that any moments or cumulants of order higher than zero cannot be defined for the Lorentzian (Cauchy distribution) function, while Lorentzian-like peak profiles are often observed, perhaps for the following reasons: (i) the spectroscopic profile of the characteristic X-ray naturally has a Lorentzian character, (ii) the size-broadening profile of small crystallites is likely to have a Lorentzian-like shape (Popa & Balzar, 2002; Ida *et al.*, 2003), and (iii) the broadening caused by stacking faults with low mutual correlation has intrinsically Lorentzian character as the result of Fourier transform of the exponential distribution of coherent domain size. Therefore, we should define alternative measures of sharpness instead of the moments or cumulants for analysis of experimental diffraction peak profiles.

Fortunately, the cumulants of the Fourier transform can be defined for most of the peak profile functions, including the Lorentzian function. The Fourier transform $F(x)$ of a real symmetric function $f(k)$ located at the origin, defined by

$$F(x) \equiv \int_{-\infty}^{\infty} f(k) \exp(2\pi i k x)\,\mathrm{d}k, \tag{6}$$

is also real and symmetric. When the profile function $f(k)$ is normalized, the value of $F(x)$ at the origin $x = 0$ becomes unity, that is, $F(0) = 1$. Since the area of the Fourier transform $F(x)$ is identical to the value $f(0)$, the integral breadth B for the normalized function $f(k)$ is related to the Fourier transform $F(x)$ by the following equation,

$$B^{-1} = \int_{-\infty}^{\infty} F(x)\,\mathrm{d}x. \tag{7}$$

A parameter C_ν, which is proportional to the width of the profile function $f(k)$, can be defined for arbitrary order of ν by the following equations:

$$C_\nu \equiv \left[B \int_{-\infty}^{\infty} |x|^\nu F(x)\,\mathrm{d}x \right]^{-1/\nu} \tag{8}$$

for $\nu \neq 0$, and

$$\begin{aligned} C_0 &\equiv \lim_{\nu\to 0} \left[B \int_{-\infty}^{\infty} |x|^\nu F(x)\,\mathrm{d}x \right]^{-1/\nu} \\ &= \exp\left[-B \int_{-\infty}^{\infty} F(x) \ln|x|\,\mathrm{d}x \right]. \end{aligned} \tag{9}$$

Note that the integral breadth B can be considered as the constant for normalization about the Fourier transform $F(x)$, as shown in equation (7). The parameter C_2 is also related to the curvature of $f(k)$ at the origin, by

$$C_2^{-2} = -(B/4\pi^2) f''(0). \tag{10}$$

It is expected that the ratio of the integral breadth B to the width parameters C_ν defined in this section, (B/C_ν), can be a measure of sharpness, similarly to (A/B) or (B/W) described in the preceding section.

3. Sharpness parameters of elementary peak profile functions

In this section, the validity of the use of (B/C_ν) defined in the preceding section as the sharpness parameter is examined by comparing several peak profiles described by elementary functions. Analytical solutions of (B/C_ν) for the Gaussian, logistic distribution, hyperbolic secant, modified Lorentzian, intermediate Lorentzian and Lorentzian functions are given in Appendix *A*.

The profiles of the normalized elementary functions with an integral breadth of unity are shown in Fig. 1. The sharpness parameters (B/W), (A/B) and (B/C_ν) of the six peak functions are listed in Table 1.

The ratios of the Fourier initial slope to the integral breadth, (A/B), are zero for all the listed functions except the Lorentzian function, while the apparent sharpness of the peak

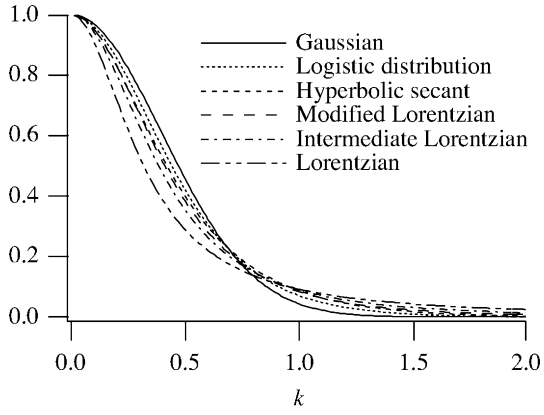

Figure 1
Profiles of normalized elementary peak profile functions: the Gaussian, logistic distribution, hyperbolic secant, modified Lorentzian, intermediate Lorentzian and Lorentzian functions.

profile shown in Fig. 1 corresponds well to the parameters (B/W) or (B/C_ν) except that the modified Lorentzian function may appear to be slightly sharper than the hyperbolic secant function, while the parameters (B/C_2) for the two functions have the same value. It is also confirmed that the curvatures of the hyperbolic secant and modified Lorentzian functions coincide at the origin, in accordance with the common value of (B/C_2) for the two functions and the relation shown in equation (10).

4. Sharpness parameters for the peak profile functions with variable shape

4.1. Voigt function

The Voigt function is defined as the convolution of the Gaussian and Lorentzian functions. When the integral breadths of the component functions are given by b_G and b_L, respectively, the convolution is expressed by

$$g_V(k; b_G, b_L) = \int_{-\infty}^{\infty} f_G(k - t; b_G) f_L(t; b_L)\, dt \qquad (11)$$

in integral formula, or by the following equations:

$$g_V(k; b_G, b_L) = b_G^{-1} V(\pi^{1/2} k/b_G, \pi^{-1/2} b_L/b_G), \qquad (12)$$

$$V(x, y) \equiv (y/\pi) \int_{-\infty}^{\infty} [y^2 + (x - t)^2]^{-1} \exp(-t^2)\, dt = \mathrm{Re}[\mathrm{wofz}(x + iy)], \qquad (13)$$

$$\mathrm{wofz}(z) \equiv \exp(-z^2)\, \mathrm{erfc}(-iz), \qquad (14)$$

where wofz(z) is a scaled complex error function called the Faddeeva function, and erfc(z) is the complementary complex error function. Re$[z]$ means the real part of the complex number z. The formulae for the normalized Gaussian and Lorentzian functions, $f_G(k; b_G)$ and $f_L(k; b_L)$, are given in equations (33) and (34) in Appendix A.

The Fourier initial slope A_V, the integral breadth B_V, and the width parameters $(C_1)_V$ and $(C_2)_V$ of the Voigt function $g_V(k; b_G, b_L)$ are given by

Table 1
Sharpness parameters for the Gaussian, logistic distribution, hyperbolic secant, modified and intermediate Lorentzian, and Lorentzian functions.

Function	B/W	A/B	$B/C_{-1/2}$	B/C_0	$B/C_{1/2}$	B/C_1	B/C_2
Gaussian	1.06447	0	0.13484	0.21138	0.26968	0.31831	0.39894
Logistic	1.13459	0	0.13770	0.22037	0.28694	0.34553	0.45016
Hyperbolic secant	1.19275	0	0.14019	0.26968	0.30290	0.37123	0.5
Modified Lorentzian	1.22033	0	0.14147	0.23142	0.30680	0.375	0.5
Intermediate Lorentzian	1.30477	0	0.14545	0.24290	0.32726	0.40529	0.55133
Lorentzian	1.57080	2	0.15916	0.28073	0.39270	0.5	0.70711

$$A_V = 2b_L,$$

$$B_V = b_G \exp(-b_L^2/\pi b_G^2)\, [\mathrm{erfc}(b_L/\pi^{1/2} b_G)]^{-1} = b_G [\mathrm{wofz}(i b_L/\pi^{1/2} b_G)]^{-1},$$

$$(C_1)_V^{-1} = \pi^{-1} b_G^{-2} (B_V - b_L),$$

$$(C_2)_V^{-1} = \pi^{-1} b_G^{-2} (\pi b_G^2/2 - b_L B_V + b_L^2)^{1/2},$$

while no simple expression for the FWHM is available.

The normalized Voigt profile for given value of integral breadth B_V can be calculated for any value of b_L/b_G as follows. A parameter defined by the following equation is introduced,

$$\rho_V \equiv b_L/(b_G + b_L), \qquad (15)$$

so that the parameter ρ_V in the range $0 \le \rho_V \le 1$ could cover all the variable shape of the Voigt profile. The parameters b_G and b_L can uniquely be determined from the parameters B_V and ρ_V by

$$b_G = B_V \exp[\pi^{-1} \rho_V^2/(1 - \rho_V)^2]\, \mathrm{erfc}[\pi^{-1/2} \rho_V/(1 - \rho_V)], \qquad (16)$$

$$b_L = b_G \rho_V (1 - \rho_V)^{-1}. \qquad (17)$$

Then the normalized Voigt profile explicitly including the integral breadth as an argument defined by the following equation,

$$f_V(k; B_V, \rho_V) \equiv g_V(k; b_G, b_L), \qquad (18)$$

can be calculated by applying equations (12), (13), (16) and (17).

The normalized Voigt profiles with an integral breadth of unity, $B_V = 1$, are plotted for $\rho_V = 0, 0.2, 0.4, \ldots, 1.0$ in Fig. 2. The component widths, b_G and b_L, for the normalized Voigt profiles and the sharpness parameters, including the parameter $(B/W)_V$ numerically evaluated by a bisection method, are also listed for $\rho_V = 0, 0.1, 0.2, \ldots, 1.0$ in Table 2.

4.2. Pearson VII function

The Pearson VII function can be expressed as

$$g_{P7}(k; \gamma_{P7}, \mu) = \pi^{-1/2} \Gamma(\mu - 1/2)^{-1} \gamma_{P7}^{-1} \Gamma(\mu) [1 + (k/\gamma_{P7})^2]^{-\mu}, \qquad (19)$$

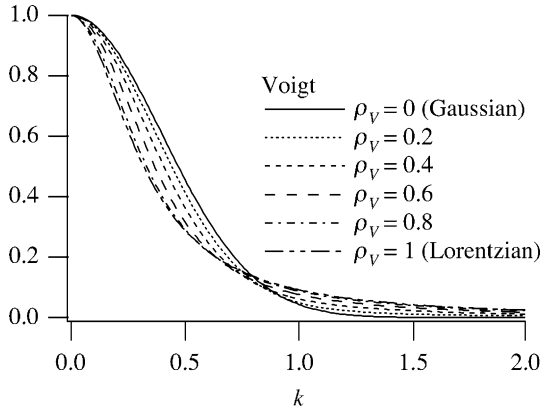

Figure 2
Profiles of the normalized Voigt function.

for $\mu > 1/2$, where γ_{P7} is a parameter proportional to the width of the peak. The parameter μ specifies the sharpness of the peak profile of the Pearson VII function. The function coincides with the Lorentzian function for $\mu = 1$, intermediate Lorentzian for $\mu = 3/2$ and modified Lorentzian for $\mu = 2$, and approaches the Gaussian function for $\mu \to \infty$. It should be noted that the Pearson VII function can model profiles sharper than the Lorentzian function for μ in the range $1/2 < \mu < 1$.

The integral breadth of the Pearson VII function B_{P7} is related to γ_{P7} as follows:

$$B_{P7} = \pi^{1/2}\Gamma(\mu)^{-1}\Gamma(\mu - 1/2)\gamma_{P7}.$$

Then the normalized Pearson VII function explicitly including the integral breadth as an argument is given by

$$f_{P7}(k; B_{P7}, \rho_{P7}) = B_{P7}^{-1}\left\{1 + \pi\left[\Gamma(\mu - 1/2)k/\Gamma(\mu)B_{P7}\right]^2\right\}^{-\mu}. \quad (20)$$

The sharpness parameter $(B/W)_{P7}$ from the FWHM of the Pearson VII function W_{P7} is related to the parameter μ by the following equation:

$$(B/W)_{P7} = (\pi^{1/2}/2)(2^{1/\mu} - 1)^{-1/2}\,\Gamma(\mu - 1/2)/\Gamma(\mu).$$

The parameter $(A/B)_{P7}$ from the Fourier initial slope A_{P7} takes only three values depending on the parameter μ as follows:

$$(A/B)_{P7} = \begin{cases} 0 & (1 < \mu) \\ 2 & (\mu = 1) \\ \infty & (1/2 < \mu < 1) \end{cases},$$

which means that the Pearson VII function can model only three types of decay in the tail of the peak profile.

The sharpness parameter for the Pearson VII function $(B/C_\nu)_{P7}$ is generally given by

$$\left(\frac{B}{C_\nu}\right)_{P7} = \frac{\Gamma(\mu - 1/2)}{\pi^{1/2}\Gamma(\mu)}\left[\frac{1}{\pi^{1/2}\Gamma(\mu)}\Gamma\left(\mu + \frac{\nu}{2}\right)\Gamma\left(\frac{\nu + 1}{2}\right)\right]^{1/\nu},$$

for any values of μ and ν in the ranges $\mu > 1/2$ and $\nu > -1$.

A shape parameter for the Pearson VII function defined by

$$\rho_{P7} \equiv \mu^{-1}$$

is introduced, so that all possible shapes of the Pearson VII function can be represented by varying the parameter ρ_{P7} within the range $0 < \rho_{P7} < 2$.

The sharpness parameters of the Pearson VII function for the values $\rho_{P7} = 0, 0.2, 0.4, \ldots, 2$ are listed in Table 3. The profiles of $f_{P7}(k; B_{P7}, \rho_{P7})$ for several values of ρ_{P7} are shown in Fig. 3. As shown in Fig. 3, the Pearson VII function for the value $1/2 < \mu < 1$ corresponds to a shape sharper than the Lorentzian profile ($\rho_{P7} = \mu = 1$). The sharpness of the Pearson VII function becomes infinite for $\mu \to 1/2$.

Table 2
Sharpness parameters for the Voigt profile.

The integral breadths of the component function, b_G and b_L, of the normalized Voigt profile with an integral breadth of unity are also listed.

ρ_V	b_G	b_L	B/W	A/B	$B/C_{-1/2}$	$B/C_{1/2}$	B/C_1	B/C_2
0	1	0	1.06447	0	0.13484	0.26968	0.31831	0.39894
0.1	0.93302	0.10367	1.09623	0.20734	0.14003	0.29041	0.32775	0.41280
0.2	0.85881	0.21470	1.13354	0.42941	0.14480	0.31134	0.33891	0.42940
0.3	0.77648	0.33278	1.17765	0.66556	0.14898	0.33155	0.35225	0.44954
0.4	0.68517	0.45678	1.22996	0.91355	0.15242	0.34991	0.36833	0.47428
0.5	0.58420	0.58420	1.29164	1.16841	0.15507	0.36536	0.38779	0.50501
0.6	0.47354	0.71031	1.36263	1.42062	0.15693	0.36536	0.41122	0.54325
0.7	0.35441	0.82695	1.43907	1.65389	0.15811	0.38521	0.43856	0.58995
0.8	0.23049	0.92196	1.50948	1.84393	0.15877	0.38992	0.46757	0.64260
0.9	0.10907	0.98164	1.55633	1.96328	0.15908	0.39213	0.49128	0.68898
1	0	1	1.57080	2	0.15916	0.39270	0.5	0.70711

4.3. Pseudo-Voigt function

The pseudo-Voigt function is given by

$$g_{pV}(k; W_{pV}, \eta) = (1 - \eta)f_G[k; (\pi/\ln 2)^{1/2}W_{pV}/2] + \eta f_L(k; \pi W_{pV}/2), \quad (21)$$

where W_{pV} is the FWHM of the function and η is the fraction of the Lorentzian component that is called the mixing parameter. The formulae for the normalized Gaussian and Lorentzian functions, $f_G(k; b_G)$ and $f_L(k; b_L)$, are given in equations (33) and (34) in Appendix *A*.

The integral breadth B_{pV} of the pseudo-Voigt function is given by

$$B_{pV} = (\pi/2)W_{pV}[(\pi \ln 2)^{1/2}(1 - \eta) + \eta]^{-1}. \quad (22)$$

Then the normalized pseudo-Voigt function can be expressed as

$$f_{pV}(k; B_{pV}, \eta) \equiv g_{pV}(k; W_{pV}, \eta), \quad (23)$$

the values of which can be calculated for any values of the integral breadth B_{pV} and the mixing parameter η by using equation (22).

The sharpness parameters of the pseudo-Voigt profile are given by

$$(B/W)_{pV} = (\pi/2)\left[(\pi \ln 2)^{1/2}(1 - \eta) + \eta\right]^{-1},$$

$$(A/B)_{pV} = 2\eta[(\pi \ln 2)^{1/2}(1 - \eta) + \eta],$$

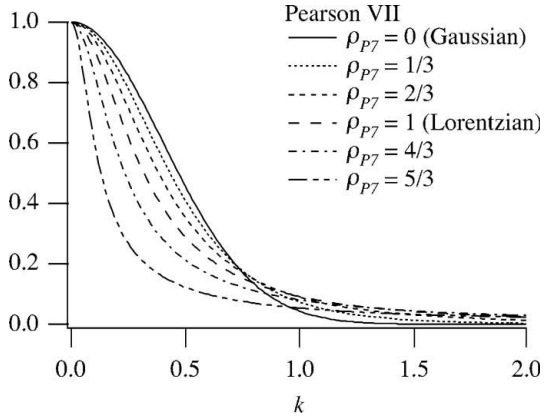

Figure 3
Profiles of the normalized Pearson VII function.

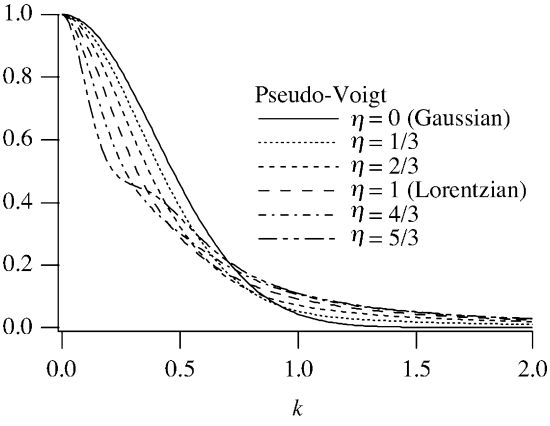

Figure 4
Profiles of the normalized pseudo-Voigt function.

$$(B/C_\nu)_{\rm pV} = [\pi^{1/2}(\ln 2)^{1/2}(1-\eta)+\eta]^{-1-1/\nu} \times \left\{(\ln 2)^{(\nu+1)/2}(1-\eta)\Gamma[(\nu+1)/2] + (\eta/2^\nu)\Gamma(\nu+1)\right\}^{1/\nu}.$$

The sharpness parameters of the pseudo-Voigt function for the values $\eta = 0, 0.2, 0.4, \ldots, 2$ are listed in Table 4. The profiles of the normalized pseudo-Voigt function with $B_{\rm pV} = 1$ and $\eta = 0, 1/3, 2/3, \ldots, 5/3$ are shown in Fig. 4.

It should be noted that the parameter $(A/B)_{\rm pV}$ has the maximum value

$$2^{-1}\pi(\ln 2)[(\pi \ln 2)^{1/2} - 1]^{-1} = 2.28899$$

at

$$\eta = 2^{-1}(\pi \ln 2)^{1/2}[(\pi \ln 2)^{1/2} - 1]^{-1} = 1.55116.$$

Practical use of the pseudo-Voigt function will be limited to the range $\eta < 1.55$, which corresponds to $(B/W)_{\rm pV} < 2.13$, $(B/C_1)_{\rm pV} < 0.72$ and $(B/C_2)_{\rm pV} < 1.11$.

The parameter η can inversely be evaluated from the sharpness parameters (B/W), (A/B), $(B/C_{-1/2})$ and (B/C_1) by solving linear or quadratic equations, while numerical solution of higher-order equations is required in the case of a general value of ν.

Table 3
Sharpness parameters for the Pearson VII profile.

$\rho_{\rm P7}$	μ	B/W	A/B	$B/C_{-1/2}$	B/C_0	$B/C_{1/2}$	B/C_1	B/C_2
0	∞	1.06447	0	0.13484	0.21138	0.26968	0.31831	0.39894
0.2	5	1.11385	0	0.13683	0.21754	0.28134	0.33646	0.43234
0.4	2.5	1.17942	0	0.13963	0.22600	0.29696	0.36025	0.47451
0.6	1.66667	1.26821	0	0.14370	0.23789	0.31838	0.39219	0.52928
0.8	1.25	1.39177	0	0.14977	0.25505	0.34854	0.43635	0.60301
1	1	1.57080	2	0.15916	0.28073	0.39270	0.5	0.70711
1.2	0.83333	1.84654	∞	0.17448	0.32136	0.46128	0.59763	0.86431
1.4	0.71429	2.31525	∞	0.20181	0.39185	0.57852	0.76301	1.12769
1.6	0.625	3.26558	∞	0.25935	0.53693	0.81719	1.09747	1.65640
1.8	0.55556	6.14089	∞	0.43801	0.98000	1.54089	2.10760	3.24623
2	0.5	∞	∞	∞	∞	∞	∞	∞

Table 4
Sharpness parameters for the pseudo-Voigt profile.

η	B/W	A/B	$B/C_{-1/2}$	B/C_0	$B/C_{-1/2}$	B/C_1	B/C_2
0	1.06447	0.00000	0.13484	0.21138	0.26968	0.31831	0.39894
0.2	1.13782	0.55221	0.13932	0.22252	0.28771	0.34342	0.43990
0.4	1.22203	1.02832	0.14402	0.23484	0.30832	0.37276	0.48852
0.6	1.31970	1.42832	0.14891	0.24850	0.33211	0.40746	0.54701
0.8	1.43434	1.75221	0.15397	0.26373	0.35988	0.44911	0.61841
1	1.57080	2.00000	0.15916	0.28073	0.39270	0.50000	0.70711
1.2	1.73594	2.17168	0.16437	0.29977	0.43210	0.56348	0.81962
1.4	1.93989	2.26726	0.16945	0.32107	0.48027	0.64475	0.96600
1.6	2.19814	2.28672	0.17415	0.34478	0.54050	0.75219	1.16250
1.8	2.53572	2.23009	0.17802	0.37075	0.61793	0.90030	1.43698
2	2.99579	2.09734	0.18035	0.39803	0.72111	1.11612	1.84099

4.4. Sharpness parameters for size-broadening profile

4.4.1. Spherical crystallite. When the shape of a crystallite is spherical, spheroidal or ellipsoidal, the size-broadening diffraction profile from the crystallite becomes identical to that of a sphere, according to the theory of Stokes & Wilson (1942). The normalized size-broadening profile is given by the following formula:

$$f_{\rm S}(k; D) = \begin{cases} 3Ds^{-2}[1 - 2s^{-1}\sin s + 4s^{-2}\sin^2(s/2)] & (k \neq 0), \\ 3D/4 & (k = 0), \end{cases} \quad (24)$$

$$s \equiv 2\pi k D, \quad (25)$$

where D is the effective dimension along the diffraction vector, which is identical to the diameter in the case of a spherical crystallite (Langford & Wilson, 1978). When the angles between the diffraction vector and the three principal axes of an ellipsoidal crystallite are α_1, α_2 and α_3, the effective dimension is given by

$$D = (D_1^{-2}\cos^2\alpha_1 + D_2^{-2}\cos^2\alpha_2 + D_3^{-2}\cos^2\alpha_3)^{-1/2}, \quad (26)$$

where the diameters along the principal directions are assumed to be D_1, D_2 and D_3 (Popa, 2005). When the diffraction vector deviates by an angle of α from the unique axis of a spheroid, the effective dimension is given by

$$D = (D_\parallel^{-2}\cos^2\alpha + D_\perp^{-2}\sin^2\alpha)^{-1/2}, \quad (27)$$

where $D_{\parallel}$ and $D_{\perp}$ are the diameters along the axial and equatorial directions, respectively.

The Fourier transform of the size-broadening profile of a spherical crystallite is given by

$$F_{\rm S}(x; D) = \begin{cases} 1 - 3|x|/2D + |x|^3/2D^3 & (|x| < D), \\ 0 & (D \leq |x|). \end{cases} \quad (28)$$

The integral breadth $B_{\rm S}$ of the function $f_{\rm S}(k; D)$ is given by

$$B_{\rm S} = (4/3)D^{-1},$$

and the sharpness parameters are given by

$$(A/B)_{\rm S} = 9/8 = 1.125,$$

$$(B/C_\nu)_{\rm S} = (4/3)\left\{8/[(\nu+1)(\nu+2)(\nu+4)]\right\}^{1/\nu}$$

for $\nu \neq 0$, and

$$(B/C_0)_{\rm S} = (4/3)\exp(-7/4) = 0.231699.$$

4.4.2. Lognormal size distribution of spherical crystallites. The density function of a lognormal distribution with a median m and logarithmic standard deviation ω is given by

$$f_{\rm LN}(D; m, \omega) = [(2\pi)^{1/2} D\omega]^{-1} \exp\{-[\ln(D/m)]^2/2\omega^2\}. \quad (29)$$

The normalized formula of diffraction intensity profiles from log-normally size-distributed crystallites is given by

$$f_{\rm SLN}(k; m, \omega) = \int_0^\infty f_{\rm S}(k; D) f_{\rm LN}[D; m\exp(3\omega^2), \omega]\,{\rm d}D, \quad (30)$$

which is abbreviated as the 'SLN' profile.

The Fourier transform of the SLN profile (Ungár *et al.*, 2001) is given by

$$\begin{aligned} F_{\rm SLN}(x; m, \omega) = {} & (1/2){\rm erfc}\{[\ln(|x|/m) - 3\omega^2]/2^{1/2}\omega\} \\ & - (3|x|/4m)\exp(-2.5\omega^2){\rm erfc}\left\{\left[\ln(|x|/m) - 2\omega^2\right]/2^{1/2}\omega\right\} \\ & + (|x|^3/4m^3)\exp(-4.5\omega^2){\rm erfc}\left\{[\ln(|x|/m)]/2^{1/2}\omega\right\}. \quad (31) \end{aligned}$$

The integral breadth $B_{\rm SLN}$ of the function $f_{\rm SLN}(k; m, \omega)$ is given by

$$B_{\rm SLN} = (4/3)m^{-1}\exp(-3.5\omega^2),$$

and the sharpness parameters are given by

$$(A/B)_{\rm SLN} = (A/B)_{\rm S}\exp(\omega^2),$$

$$(B/C_\nu)_{\rm SLN} = (B/C_\nu)_{\rm S}\exp\left[(\nu+1)\omega^2/2\right].$$

4.4.3. Approximation with the pseudo-Voigt function to the SLN profile. When the size distribution of crystallites is modelled by the log-normal distribution, the line-width and the sharpness parameters of the size-broadening profile uniquely determine all of the characteristics of the statistical distribution.

Sánchez-Bajo *et al.* (2006) have proposed the use of the pseudo-Voigt function instead of the theoretical size-broadening profile in least-squares curve fitting analysis. The mixing parameter η of the pseudo-Voigt function has been empirically related to the logarithmic standard deviation parameter ω of the log-normal distribution.

Table 5
Logarithmic standard deviation ω of the SLN profiles with integral breadth B and sharpness parameter (B/C_ν) equivalent to the pseudo-Voigt function, with the mixing parameter $\eta = 0.8, 1, 1.2$, varied on the order ν.

ν	ω ($\eta = 0.8$)	ω ($\eta = 1$)	ω ($\eta = 1.2$)
−2	0.66566	0.75853	0.81100
−3/2	0.60068	0.70675	0.77651
−1	0.55837	0.67039	0.75425
−1/2	0.52936	0.64238	0.73587
0	0.50886	0.61961	0.71772
1/2	0.49410	0.60043	0.69857
1	0.48332	0.58389	0.67857
3/2	0.47532	0.56935	0.65839
2	0.46927	0.55639	0.63876

As has been previously reported (Ida *et al.*, 2003), the SLN profile will become close to the Lorentzian profile when the value of the logarithmic standard deviation ω in determining the sharpness of the profile has certain values corresponding to similar sharpness as the Lorentzian function.

Sánchez-Bajo *et al.* (2006) have suggested that the SLN profile with the least-squares deviation from the Lorentzian function corresponds to $\omega = 0.70$, while the values of ω evaluated through sharpness parameters equivalent to the Lorentzian function are given by

$$\omega = [2\ln(4/3)]^{1/2} = 0.758528$$

for the same (A/B),

$$\omega = [(7/2) + 2\ln(3/8) - 2\gamma]^{1/2} = 0.619605$$

for the same (B/C_0), and

$$\omega = \left\{\frac{2}{\nu+1}\left[\ln\frac{3}{8} + \frac{1}{\nu}\ln\frac{(\nu+4)\Gamma(\nu+3)}{8}\right]\right\}^{1/2}$$

for the same (B/C_ν) with $\nu \neq 0$. The above relations clearly show that the parameters for the 'Lorentzian-like' SLN profile depend on the definition of the sharpness parameter.

The variation of ω for 'Lorentzian-like' profiles evaluated through (B/C_ν) is listed in the third column of Table 5, where the values for the equal sharpness to the pseudo-Voigt function with $\eta = 0.8$ and $\eta = 1.2$ are also listed in the second and fourth columns. The values of ω corresponding to $\nu = -2, -1$ are numerically evaluated as the limit values for $\nu \to -2, -1$.

Fig. 5 compares the pseudo-Voigt functions for the mixing parameters (*a*) $\eta = 0.8$, (*b*) $\eta = 1$ (Lorentzian) and (*c*) $\eta = 1.2$ with the SLN profiles that have the equivalent integral breadth and sharpness parameters for $\nu = -3/2, -1/2, 1/2, 3/2$. The difference curves show the tendency that the deviation in the tail and peak regions is greater for smaller and larger values of ν, respectively. It is suggested that a value around $\nu = -1/2$ gives the minimum deviation on the approximation of the SLN profile by the pseudo-Voigt function through the sharpness parameter (B/C_ν), and the uncer-

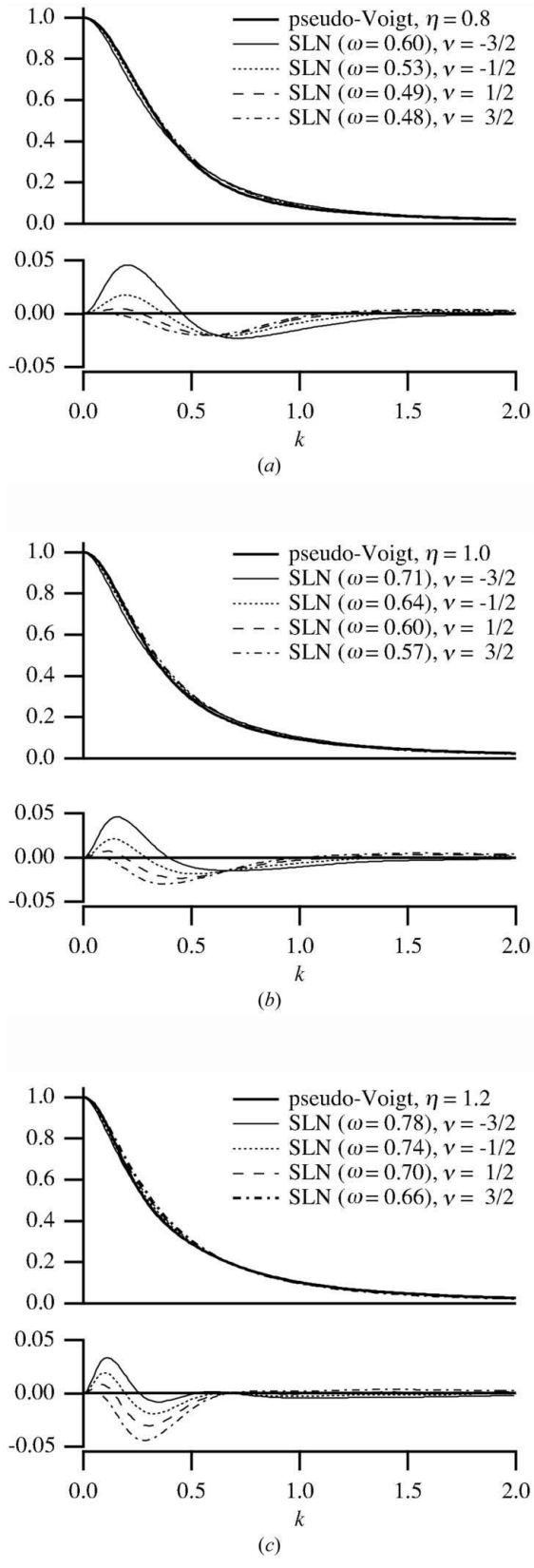

Figure 5
Comparison of the pseudo Voigt functions for the mixing parameters (*a*) $\eta = 0.8$, (*b*) $\eta = 1$ (Lorentzian) and (*c*) $\eta = 1.2$ with the SLN profile functions with equivalent integral breadth and sharpness parameters (B/C_ν) for $\nu = -3/2, -1/2, 1/2, 3/2$. Difference curves are plotted in the lower part of each panel.

Table 6
Profile parameters of the SLN profile function optimized by a least-squares method to fit the pseudo-Voigt functions defined in different data ranges.

	Range (I), $\|x\| < 2B$			Range (II), $\|x\| < 4B$			Range (III), $\|x\| < 6B$		
	$\eta = 0.8$	$\eta = 1$	$\eta = 1.2$	$\eta = 0.8$	$\eta = 1$	$\eta = 1.2$	$\eta = 0.8$	$\eta = 1$	$\eta = 1.2$
b_0	0.0078	0.0070	−0.0008	0.0022	0.0020	0.0007	0.0010	0.0009	0.0004
S	0.943	0.944	0.996	0.971	0.973	0.988	0.980	0.982	0.990
m	0.695	0.405	0.181	0.578	0.326	0.192	0.534	0.298	0.180
ω	0.449	0.599	0.760	0.501	0.646	0.750	0.523	0.665	0.755

tainty in the evaluated ω will be within about ± 0.1, independent of the order ν of the sharpness parameter (B/C_ν).

Finally, ambiguity about the least-squares-based optimization of approximation with empirical functions for theoretical profiles, which has been commonly adopted in the literature treating this subject (Thompson *et al.*, 1987; Ida *et al.*, 2000; Popa & Balzar, 2002; Sánchez-Bajo *et al.*, 2006), is briefly discussed. Table 6 lists the results of least-squares fitting by the SLN profile to the pseudo-Voigt functions with the integral breadth of unity ($B = 1$) and the mixing parameters $\eta = 0.8, 1, 1.2$. Three different data sets in the ranges $|x| < 2B$ (I), $|x| < 4B$ (II) and $|x| < 6B$ (III) are separately analysed. A model function of the following form is applied:

$$f(x) = b_0 + Sf_{\rm SLN}(x; m, \omega), \tag{32}$$

where the constant background b_0, integrated intensity S, median diameter m and logarithmic standard deviation ω in the SLN profile function are treated as the adjustable parameters. As is listed in Table 6, the optimized values of the parameters vary considerably in the data range for the analysis. Furthermore, it is expected that the results of the least-squares fitting will also be affected by the background level and assumed statistics, when it is applied to experimentally obtained diffraction peak intensity profiles.

The concept of approximation through the sharpness parameter (B/C_ν) seems favourable because of the unambiguous definition of formulae and the portability to various model function systems, including theoretical size-broadening profiles with statistical distribution.

5. Conclusion

A new definition of the sharpness parameter, which is defined through the νth-order moment of the Fourier transform, for symmetric peak profile functions has been examined. Analytical expressions for the sharpness parameter for empirical model profile functions, namely the Gaussian, logistic distribution, hyperbolic secant, Lorentzian, Voigt, Pearson VII and pseudo-Voigt functions, and theoretical size-broadening profiles with statistical size distribution have been derived. Theoretical diffraction profiles of spherical crystallites with log-normal size distribution can be approximated by the pseudo-Voigt function with equivalent values of the sharpness parameter for $\nu = -1/2$. The concept of the sharpness parameter will provide a simple way to define an approximation

for theoretical diffraction peak profile by empirical model functions.

APPENDIX *A*
Analytical expressions of elementary peak profile functions

A1. Gaussian function

The normalized Gaussian function with integral breadth B_G is given by

$$f_G(k; B_G) = B_G^{-1} \exp(-\pi k^2/B_G^2). \quad (33)$$

The sharpness parameters from the FWHM W and Fourier initial slope A of the Gaussian function are given by

$$(B/W)_G = 2^{-1}\pi^{1/2}(\ln 2)^{-1/2} = 1.06447,$$

$$(A/B)_G = 0.$$

The sharpness parameters $(B/C_\nu)_G$ of the Gaussian function are given by

$$(B/C_\nu)_G = \pi^{-(1+1/\nu)/2}\left\{\Gamma[(\nu+1)/2]\right\}^{1/\nu},$$

for $\nu \neq 0$, where $\Gamma(x)$ is the gamma-function defined by

$$\Gamma(x) \equiv \int_0^\infty t^{x-1}\exp(-t)\,dt. \quad (34)$$

The values for $\nu = -1/2, 0, 1/2, 1, 2$ are given by

$$(B/C_{-1/2})_G = \pi^{1/2}[\Gamma(1/4)]^{-2} = 0.134838,$$

$$(B/C_0)_G = 2^{-1}\pi^{-1/2}\exp(-\gamma/2) = 0.211375,$$

$$(B/C_{1/2})_G = \pi^{-3/2}[\Gamma(3/4)]^2 = 0.269676,$$

$$(B/C_1)_G = \pi^{-1} = 0.318310,$$

$$(B/C_2)_G = (2\pi)^{-1/2} = 0.398942,$$

where γ is the Euler constant, defined by

$$\gamma \equiv \lim_{n\to\infty}\left(\sum_{j=1}^{n} j^{-1} - \ln n\right) = 0.57721566490153286060\ldots,$$

A2. Logistic distribution function

The logistic distribution function is equivalent to the square of the hyperbolic secant function defined by

$$\mathrm{sech}(x) \equiv 2[\exp(x) + \exp(-x)]^{-1}.$$

The normalized formula for the logistic distribution function with the integral breadth B_{SH2} is given by

$$f_{SH2}(k; B_{SH2}) = B_{SH2}^{-1}\mathrm{sech}^2(2k/B_{SH2}). \quad (35)$$

The sharpness parameters (B/W) and (A/B) for the function are given by

$$(B/W)_{SH2} = \left[\ln(2^{1/2}+1)\right]^{-1} = 1.13459,$$

$$(A/B)_{SH2} = 0.$$

Although a simple expression of (B/C_ν) for the general value of ν is not always available, some analytical solutions for integer or half-integer values of ν are as follows:

$$(B/C_{-1/2})_{SH2} = \pi\left[\zeta\left(\frac{3}{2},\frac{1}{2}\right)\right]^{-2} = 0.137697,$$

$$(B/C_0)_{SH2} = \frac{2}{\pi^2}\exp\left[\frac{4}{\pi^2}\int_0^\infty \frac{t\ln t}{\sinh t}\,dt\right] = 0.220372,$$

$$(B/C_1)_{SH2} = \frac{9}{4\pi^5}\left[\zeta\left(\frac{5}{2},\frac{1}{2}\right)\right]^2 = 0.28694,$$

$$(B/C_1)_{SH2} = 28\pi^{-4}\zeta(3) = 0.345528,$$

$$(B/C_2)_{SH2} = 2^{1/2}\pi^{-1} = 0.450158,$$

where $\zeta(s)$ is the Riemann Zeta function defined by

$$\zeta(s) \equiv \sum_{k=1}^{\infty} k^{-s},$$

and $\zeta(s, \nu)$ is the Hurwitz Zeta function (generalized Riemann Zeta function) defined by

$$\zeta(s,\nu) \equiv \sum_{k=0}^{\infty}(\nu+k)^{-s}.$$

A3. Hyperbolic secant function

The normalized hyperbolic secant function with the integral breadth B_{SH} is given by

$$f_{SH}(k; B_{SH}) = B_{SH}^{-1}\,\mathrm{sech}\,(\pi k/B_{SH}). \quad (36)$$

The sharpness parameters for the function are given by

$$(B/W)_{SH} = \pi/[2\ln(2+3^{1/2})] = 1.19275,$$

$$(A/B)_{SH} = 0,$$

$$(B/C_{-1/2})_{SH} = \frac{1}{4}\left[\zeta\left(\frac{1}{2},\frac{1}{4}\right) - \zeta\left(\frac{1}{2},\frac{3}{4}\right)\right]^{-2} = 0.140194,$$

$$(B/C_0)_{SH} = \pi^{-1}\exp\left[\gamma - \frac{4}{\pi}\sum_{k=0}^{\infty}\frac{(-1)^k\ln(1+2k)}{1+2k}\right] = 0.228473,$$

$$(B/C_{1/2})_{SH} = \frac{1}{16\pi^2}\left[\zeta\left(\frac{3}{2},\frac{1}{4}\right) - \zeta\left(\frac{3}{2},\frac{3}{4}\right)\right]^2 = 0.302896,$$

$$(B/C_1)_{SH} = 4\pi^{-2}\mathrm{G} = 0.371227,$$

$$(B/C_2)_{SH} = 2^{-1} = 0.5,$$

where G is the Catalan constant given by

$$\mathrm{G} \equiv \sum_{k=0}^{\infty}(-1)^k(2k+1)^{-1} = 0.915965594177\ldots,$$

A4. Modified and intermediate Lorentzian functions

The modified and intermediate Lorentzian functions are special cases of the Pearson VII function (Young & Wiles, 1982).

The normalized formula of the modified Lorentzian function for integral breadth B_{ML} is given by

$$f_{\mathrm{ML}}(k; B_{\mathrm{ML}}) = B_{\mathrm{ML}}^{-1}(1 + \pi^2k^2/4B_{\mathrm{ML}}^2)^{-2}. \quad (37)$$

The sharpness parameters for the modified Lorentzian function are

$$(B/W)_{\mathrm{ML}} = (\pi/4)(2^{1/2} - 1)^{-1/2} = 1.22033,$$

$$(A/B)_{\mathrm{ML}} = 0,$$

$$(B/C_\nu)_{\mathrm{ML}} = (1/2)\left\{\pi^{-1/2}\Gamma(\nu/2 + 2)\Gamma[(\nu+1)/2]\right\}^{1/\nu},$$

for $\nu \neq 0$, and

$$(B/C_0)_{\mathrm{ML}} = (1/4)\exp(1/2 - \gamma) = 0.231423.$$

The normalized formula of the intermediate Lorentzian function for integral breadth B_{IL} is given by

$$f_{\mathrm{IL}}(k; B_{\mathrm{IL}}) = B_{\mathrm{IL}}^{-1}(1 + 4k^2/B_{\mathrm{IL}}^2)^{-3/2}. \quad (38)$$

The sharpness parameters for the intermediate Lorentzian function are given by

$$(B/W)_{\mathrm{IL}} = (2^{2/3} - 1)^{-1/2} = 1.30477,$$

$$(A/B)_{\mathrm{IL}} = 0,$$

$$(B/C_\nu)_{\mathrm{IL}} = 2\pi^{-1}\left\{2\pi^{-1}\,\Gamma[(\nu+3)/2]\,\Gamma[(\nu+1)/2]\right\}^{1/\nu}$$

for $\nu \neq 0$, and

$$(B/C_0)_{\mathrm{IL}} = 2^{-1}\pi^{-1}\exp(1 - \gamma) = 0.242903,$$

A5. Lorentzian function

The normalized Lorentzian function with integral breadth B_{L} is given by

$$f_{\mathrm{L}}(k; B_{\mathrm{L}}) = B_{\mathrm{L}}^{-1}(1 + \pi^2k^2/B_{\mathrm{L}}^2)^{-1}. \quad (39)$$

The sharpness parameters from the FWHM and Fourier initial slope are given by

$$(B/W)_{\mathrm{L}} = \pi/2 = 1.5708,$$

$$(A/B)_{\mathrm{L}} = 2.$$

The sharpness parameters $(B/C_\nu)_{\mathrm{L}}$ of the Lorentzian function are given for general values of ν by

$$(B/C_\nu)_{\mathrm{L}} = 2^{-1}[\Gamma(\nu+1)]^{1/\nu},$$

for $\nu \neq 0$; the values for $\nu = -1/2, 0, 1/2, 1, 2$ are

$$(B/C_{-1/2})_{\mathrm{L}} = 2^{-1}\pi^{-1} = 0.159155,$$

$$(B/C_0)_{\mathrm{L}} = 2^{-1}\exp(-\gamma) = 0.28073,$$

$$(B/C_{1/2})_{\mathrm{L}} = 8^{-1}\pi = 0.392699,$$

$$(B/C_1)_{\mathrm{L}} = 2^{-1} = 0.5,$$

$$(B/C_2)_{\mathrm{L}} = 2^{-1/2} = 0.707107.$$

References

Ida, T., Ando, M. & Toraya, H. (2000). *J. Appl. Cryst.* **33**, 1311–1316.
Ida, T., Shimazaki, S., Hibino, H. & Toraya, H. (2003). *J. Appl. Cryst.* **36**, 1107–1115.
Langford, J. I., Louër, D. & Scardi, P. (2000). *J. Appl. Cryst.* **33**, 964–974.
Langford, J. I. & Wilson, A. J. C. (1978). *J. Appl. Cryst.* **11**, 102–113.
Popa, N. C. (2005). XX Congress of the International Union of Crystallography, Florence, Italy.
Popa, N. C. & Balzar, D. (2002). *J. Appl. Cryst.* **35**, 338–346.
Sánchez-Bajo, F., Ortiz, A. L. & Cumbrera, F. L. (2006). *Acta Mater.* **54**, 1–10.
Stokes, A. R. & Wilson, A. J. C. (1942). *Proc. Camb. Philos. Soc.* **38**, 312–322.
Thompson, P., Cox, D. E. & Hastings, J. B. (1987). *J. Appl. Cryst.* **20**, 79–83.
Ungár, T., Gubicza, J., Ribárik, G. & Borbély, A. (2001). *J. Appl. Cryst.* **34**, 298–310.
Warren, B. E. (1969). *X-ray Diffraction*. New York: Dover.
Williamson, G. K. & Hall, W. H. (1953). *Acta Metall.* **1**, 22–31.
Young, R. A. & Wiles, D. B. (1982). *J. Appl. Cryst.* **15**, 430–438.